International Journal of Innovative Computing, Information and Control
Volume **18**, Number **3**, June **2022**

ICIC International ©2022 ISSN 1349-4198
pp. 1009–1018

A VALIDATION ANALYSIS OF THE SUBMILLIMETER-WIDTH CONCRETE CRACK DETECTION BASED ON MORPHOLOGICAL COMPONENT ANALYSIS AND ANISOTROPIC DIFFUSION

Ankur Dixit[1], Wataru Oshiumi[1] and Hiroaki Wagatsuma[1,2]

[1]Graduate School of Life Science and Systems Engineering
Kyushu Institute of Technology (Kyutech)
2-4 Hibikino, Wakamatsu-Ku, Kitakyushu 808-0196, Japan
ankur.dixit003@gmail.com; oshiumi.wataru745@mail.kyutech.jp; waga@brain.kyutech.ac.jp

[2]RIKEN Center for Brain Science (RIKEN CBS)
2-1 Hirosawa, Wako, Saitama 351-0198, Japan

Received September 2021; revised December 2021

Abstract. *Abnormality detection in an early stage is a crucial issue to maintain social concrete infrastructures. The submillimeter-width concrete crack detection is the inevitable mission to significantly reduce the human burden; however, conventional image processing methods do not reach the same level of human inspections in senses of coverage ratios and hit rates. In the present study, we hypothesized that a concrete crack detection based on the morphological component analysis (MCA) can be upgraded with after-treatments for contrast enhancements by using anisotropic diffusion and related techniques, to be able to detect cracks on images even for less than 10 pixels in width as a submillimeter range. The traditional MCA method was modified to decompose the image into its coarse and fine components and the coefficient of anisotropic diffusion was designed to find cracks in high gradient and low gray level regions. The modified MCA and anisotropic diffusion with the Sobel edge detector were embedded to a consistent workflow to detect submillimeter cracks in image. In the accuracy verification, comparisons among the proposed method, conventional methods and the human detection demonstrated that the proposed method had a noteworthy detection efficiency with high coverage ratios and hit rates over 60% in total. It can contribute to the actual field work of the concrete crack detection.*

Keywords: Anisotropic diffusion, Coverage ratio, Crack detection, Edge detection, Hit rate, Image morphology, Morphological component analysis, Wavelet transform

1. **Introduction.** In the image processing, linear filters, such as Gabor filters, have conventionally used for texture analyses and anomaly detections. The crack detection in the surface of buildings and others in the social infrastructure is highly important for preventive maintenance in sustainable public administration and an automatic detection was expected as Salman et al. [1] demonstrated the Gabor filter to apply the pavement crack detection. Recently, machine learning and neural network models [2, 3, 4] have studied for crack pattern analyses. It is the right direction in the sense of the generalization of image recognition. However, since they are discrete pixel-based pattern recognition methods, it has the inevitable limitation if the crack width is getting thinner than a few pixels, as a sub-millimeter level detection. In the recent trend, the sub-millimeter crack detection is an urgent mission for government and public administration, because the lifetime of concrete buildings in the social infrastructure has almost passed commonly in developed countries. As the alternative direction, wavelet transform-based methods have studied

DOI: 10.24507/ijicic.18.03.1009

for anomaly detections in continuous change of signals, independent of pixel-based discretizations in principle [5], known as multiresolution analysis to be robust against image resolution issues. Therefore, in the field data analysis with a certain quality assurance, wavelet transform-based methods were implemented as a trusty method [6, 7], instead of human expert inspections. On the other hand, it has drawbacks in the sense of the automation of parameter settings and mother wavelet selections and then system engineers have to tune parameters and other settings to maximize its performance, i.e., lower generality than learning model schemes.

In the aim of overcoming the drawback, morphological component analysis (MCA) [8, 9, 10] was proposed to automate the parameter tuning and selection of the best wavelet basis for a fine texture analysis. MCA algorithm contains an iterative process to turn internal parameters acting as an adaptive thresholding [11], conceptually similar to the learning scheme in a part. It was unclear that MCA works well for the crack detection and Dixit and Wagatsuma [12, 13] preliminarily demonstrated its performance. However, they suggested that improvements are necessary for a fine sub-millimeter crack detection if it is a pure MCA scheme. It implies that an after-treatment of decomposed textural characteristics in MCA is important to assure the quality of the detection, and then a contrast enhancement of alternative factors is necessary for coarse/fine and rough/smooth components. In the present study, for overcoming of drawbacks completely, the traditional MCA algorithm was upgraded by the integration with SWT (stationary wavelet transform) and DWT (discrete wavelet transform) to enhance coarse/fine contrasts and modified anisotropic diffusion and the Sobel edge detector to enhance rough/smooth contrasts for an enriched capability to find small sized cracks in the image.

The remainder of this paper is organized as follows. After giving brief introduction of the present study in Section 1, Section 2 described the upgrading method of MCA. Section 3 described the experimental setup for crack detection. Results of computer experiments and conclusion including discussion were respectively described in Section 4 and Section 5.

2. MCA-Based Proposed Method.

2.1. Basics of MCA algorithm.

For any x, which is a linear combination of K signals as $x = \sum_{i=1}^{K} x_i$, where each x_i represents a different type of signals to be decomposed, MCA considers an overcomplete dictionary $\phi_i \in \mathbf{M}^{N \times L_i}$ (where ϕ_i are basis elements of a dictionary $\boldsymbol{\phi}$) in which for every i, x_i is sparse in ϕ_i and it is not sparse in other ϕ_j $(\forall i \neq j)$ and $\left\|\phi_i^T x_i\right\|_0 < \left\|\phi_j^T x_j\right\|_0$, where $||b||_0$ represents the number of non-zero coefficients in b, i.e., l_0 *pseudo-norm* of vector b [9].

For simplicity, an image I (the original image) is assumed to be the linear combination of two morphological components, i.e., $I = \sum_{i=1}^{2} I_i$, where I_1 and I_2 respectively denote texture and natural components of the original image. The image $I_{j=1,2}$ can be decomposed in $\alpha_{j=1,2}$ as follows:

$$\alpha_{j=1,2} = \phi_{j=1,2}^T I_{j=1,2}, \tag{1}$$

where α_1 and α_2 respectively denote coefficients of texture and natural components. For the image I to find the sparse representation of texture and natural components over the combined dictionary ϕ, following equations have to be solved:

$$\begin{aligned} \left\{\alpha_1^{opt}, \alpha_2^{opt}\right\} &= \arg \min_{\{\alpha_1, \alpha_2\}} ||\alpha_1||_0 + ||\alpha_2||_0, \\ \text{Subject to: } I &= \phi_1 \alpha_1 + \phi_2 \alpha_2. \end{aligned} \tag{2}$$

On the other hand, the problem formulated in Equation (2) is non-convex and it is hard to solve normally, because the equation complexity grows exponentially with the number of columns in dictionary. The basis pursuit (BP) algorithm [14] was proposed to replace l_0-*norm* with l_1-*norm* for solving this issue. By replacing l_0-*norm* with l_1-*norm* to be a tractable convex optimization problem from Equation (2), the equation becomes a solvable problem to find morphological coefficients as follows:

$$\begin{aligned} &\left\{\alpha_1^{opt}, \alpha_2^{opt}\right\} = \arg\min_{\{\alpha_1,\alpha_2\}} ||\alpha_1||_1 + ||\alpha_2||_1, \\ &\text{Subject to: } I = \phi_1\alpha_1 + \phi_2\alpha_2, \end{aligned} \tag{3}$$

where $||b||_1$ represents l_1 *pseudo-norm* of vector b.

For a noisy image, it is known that sparse texture and natural components are difficult to decompose as Fuchs [15] discussed, and therefore the following version of BP was proposed to obtain the sparse morphological components of a noisy image:

$$\begin{aligned} &\left\{\alpha_1^{opt}, \alpha_2^{opt}\right\} = \arg\min_{\{\alpha_1,\alpha_2\}} ||\alpha_1||_1 + ||\alpha_2||_1, \\ &\text{Subject to: } ||I - \phi_1\alpha_1 - \phi_2\alpha_2||_2 < \epsilon, \end{aligned} \tag{4}$$

where $||b||_2$ represents l_2-*norm* of vector b and ϵ denotes the noise level in image I. For an improvement of the separation process with a reduction of the ringing artifacts in the image, a total variation (TV) regularization term was recommended to add [9, 10]. After adding TV regularization term, Equation (4) becomes as follows:

$$\left\{\alpha_1^{opt}, \alpha_2^{opt}\right\} = \arg\min_{\{\alpha_1,\alpha_2\}} ||\alpha_1||_1 + ||\alpha_2||_1 + \mu||I - \phi_1\alpha_1 - \phi_2\alpha_2||_2^2 + \gamma TV\{\phi_1\alpha_1\}. \tag{5}$$

In Equation (5), the term $\gamma TV\{\phi_1\alpha_1\}$ contributes to the computation of the piecewise texture component $\{I_1 = \phi_1\alpha_1\}$ and the separation process (μ is a scaling factor used for the noise reducing coefficient in this case). By taking two dictionaries $\phi = [\phi_1, \phi_2]$ as discrete sin transform and local discrete cosine transform [9, 10, 16], Starck et al. [9, 10] proposed an algorithm to solve Equation (5), which decomposes the given image I into its texture and natural parts [15]. As a drawback of the traditional MCA algorithm, it is capable of decomposing the single texture component (I_1) with respect to the natural component (I_2), while other components may drop out if it contains multiple and diverse texture characteristics. For the improvement of the traditional MCA algorithm, we focused on the decomposition of coarse and fine components and the modified version can be considered.

2.2. **Modified MCA algorithm as proposal.** For removing the concern due to the restriction of dictionaries in the traditional MCA, additional dictionaries can be assumed to decompose the image into its coarse and fine components. Therefore, the modified MCA was designed to pursue more than the single texture characteristic of the image. The formulation of Equation (5) was modified to contain additional dictionary parameters as follows:

$$\begin{aligned} &\left\{\alpha_c^{opt}, \alpha_f^{opt}, T_c^{opt}, T_f^{opt}\right\} \\ &= \arg\min_{\{\alpha_c,\alpha_f,T_c,T_f\}} \left\|\alpha_c T_c^{opt}\right\|_1 + \left\|\alpha_f T_f^{opt}\right\|_1 + \|I - \alpha_c - \alpha_f\|_2^2 + \gamma TV\{T_c\alpha_c\}, \end{aligned} \tag{6}$$

where T_c^{opt} and T_f^{opt} respectively denote transformation filters (dictionaries) to extract coarse and fine components. α_c and α_f respectively denote coarse and fine components of the image. Algorithm 1 was used to solve Equation (6) for the decomposition of the image into its coarse and fine components, where $Iter_{\max}$ is the maximum number of iterations, μ_c and μ_f are uniformly decreased to zero when obtaining an optimized result. λ is a

Algorithm 1. Modified MCA algorithm to decompose image into its coarse and fine components

Step 1. (a) Initialize $Iter_{\max}$, stopping threshold for image separation.
(b) Initialize μ_c and μ_f, parameters for dictionary of coarse component T_c and dictionary of fine component T_f respectively.
(c) Set $\delta = \lambda$ and σ as threshold values for updating parameters of the dictionaries.
(d) Set α_c and $\alpha_f = 0$.
Step 2. For $i = 1 : Iter_{\max}$
Update α_c assuming α_f is fixed:
– Calculate the residual $r = I - \sum_{j=c,f} \alpha_j$.
– Calculate the transformation T_c of $\alpha_c + r$ and obtain $\alpha_c' = T_c(\alpha_c + r)$
– Calculate $d = \|\alpha_c' - \alpha_c\|_1$
– If $d > \sigma$, update T_c by updating μ_c with $\mu_c = \mu_c - \frac{\mu_c}{Iter_{\max}}$.
Else, μ_c keep the same value.
– Update α_c with α_c'
Update α_f assuming α_c is fixed:
– Calculate the residual $r = I - \sum_{j=c,f} \alpha_j$.
– Calculate the transformation T_f of $\alpha_f + r$ and obtain $\alpha_f' = T_f(\alpha_f + r)$
– Calculate $d = \left\|\alpha_f' - \alpha_f\right\|_1$
– If $d > \sigma$, update T_f by updating μ_f with $\mu_f = \mu_f - \frac{\mu_f}{Iter_{\max}}$.
Else, μ_f keep the same value.
– Update α_f with α_f'
Step 3. Update the threshold by $\delta = \delta - \lambda$.
Step 4. If $\delta > \lambda$, return to step 2 else finish.

noise deducting coefficient and scaling constant to determine the relative importance of these two sparse coefficients.

2.3. **Modified anisotropic diffusion as proposal.** For the images containing cracks, background pixels and pixels to represent a crack (crack pixels) may have similar gradients on the surface of image. The anisotropic diffusion model [17] may have a potential to discriminate those minor differences, while an effective allocation of weights to be smooth in individual pixels of the image is necessary for the purpose.

According to high gradient magnitude and low gray level components in the image, diffusion coefficients of the conventional diffusion model were improved to integrate gradient magnitude and gray level variance for adaptive smoothing. The new set of diffusion coefficients was proposed to obtain crack pixels in image as follows:

$$d(\nabla I, g) = \frac{1}{1 + \left[g(x,y) \cdot \left(\frac{\bar{K}}{\nabla I(x,y)} \right)^2 \right]}, \tag{7}$$

where

$$\bar{K} = \frac{\ln(k)}{k}, \quad g(x,y) = \frac{255 \cdot I_0(x,y)}{255 + \nabla I(x,y)}. \tag{8}$$

Here, $\bar{K}$ is a new constant and acts as an edge strength threshold regularization parameter and k is an edge magnitude parameter defined in the conventional diffusion model. The

8-bit display normalized gray level of an original image $I_0(x, y)$ is defined by $g(x, y)$. ∇I is the gradient of image I and '$a \cdot b$' represents the product of a and b. The diffusion coefficient $d(\nabla I, g)$ defined in Equation (7) works as well as the diffusion coefficient defined in the conventional diffusion model [17].

The proposed diffusion coefficient function in Equation (7) forms an inverse quadratic function. It indicates that the diffusion coefficient $d(\nabla I, g)$ is directly proportional to gradient values of the image as $\nabla I(x, y)$ and inversely proportional to normalized gray value as $g(x, y)$. Thus, values of diffusion coefficients are high for pixels having high gradients and low gray levels, while the values are low for pixels having low gradients and high gray levels.

2.4. **Proposed model for crack detection.** The presence of cracks on the bridge surface is one of the important information for risk managements. Large cracks on the surface are easily identified by human inspectors even from a distant place. On the other hand, some crack width is very thin and it requires to identify in a close range, which is tough for human inspectors especially in bridges and high places. A drone-based inspection method is possible to use high proximity cameras for inspecting the surface of the bridge, which is able to record images in video associated with locational information. The remaining problem is finding cracks in images and then we designed the image processing procedure.

Figure 1 shows the workflow with modified MCA (Section 2.2) and modified anisotropic diffusion (Section 2.3). Remarked steps are visualized by example images in each step

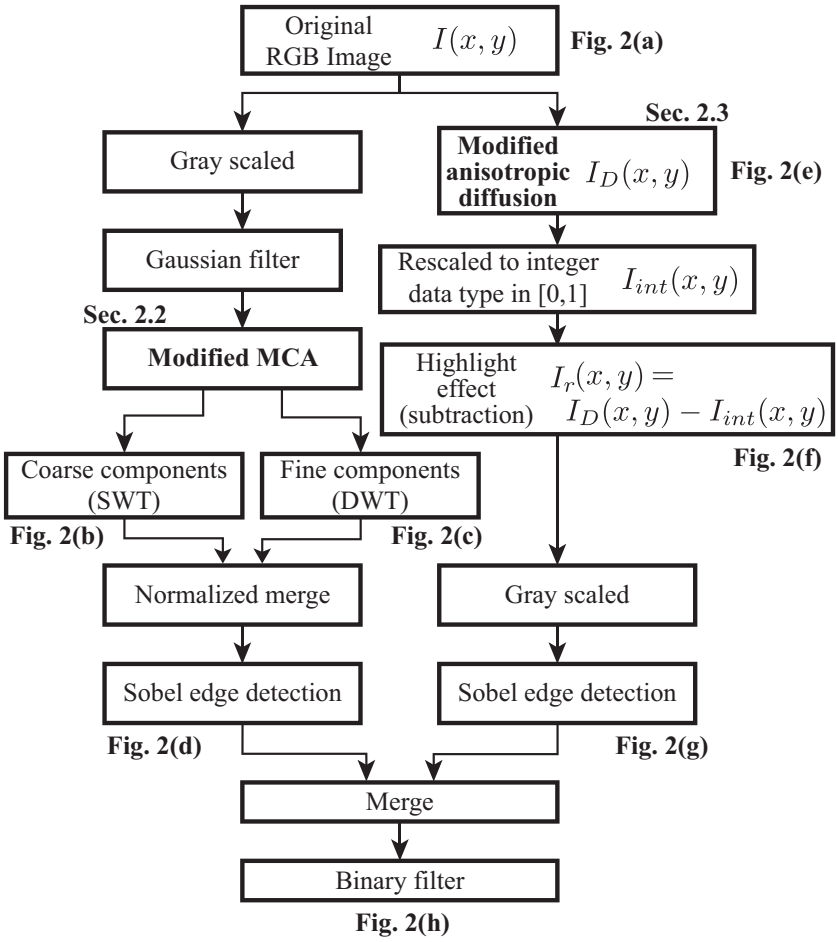

FIGURE 1. The crack detection workflow of image processing with modified MCA and modified anisotropic diffusion

shown in Figure 2, which correspond to steps in Figure 1 referred by individual subfigure numbers. We designed the whole procedure to embed the after-treatment of decomposed textural characteristics in MCA to assure the quality of the detection and the proper contrast enhancement of alternative factors for coarse/fine and rough/smooth components. We hypothesized that the traditional MCA algorithm can overcome the drawbacks by the integration with SWT and DWT to enhance coarse/fine contrasts and merge with the output from modified anisotropic diffusion to enhance rough/smooth contrasts for an enriched capability to find thin cracks.

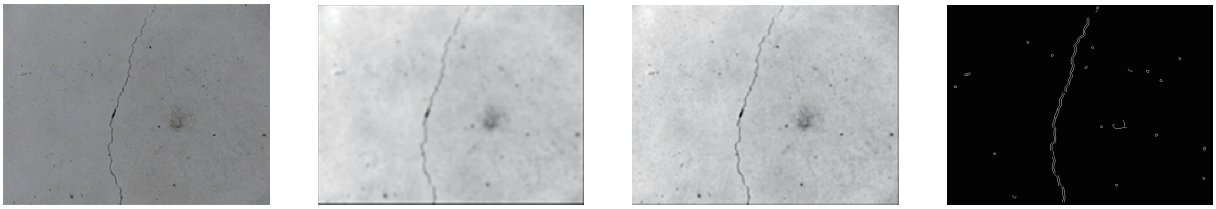

(a) Original image (b) Coarse components decomposition (c) Fine components decomposition (d) Crack detection result by MCA

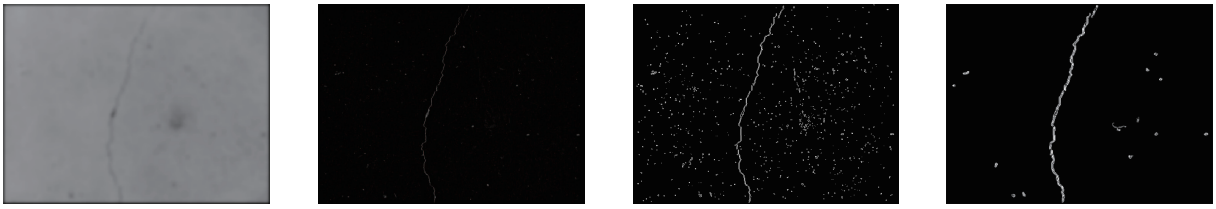

(e) Diffused image obtained by AD (f) Results after subtraction (g) Crack detection result by AD (h) Final result after binary filtering

FIGURE 2. Steps involved for cracks detection in image

3. **Experimental Setup.** In the present study, we have used a drone with high proximity camera installed on it to make a video of essential parts of the bridge as shown in Figure 3. This video was converted into the set of images and the crack detection workflow was applied in an off-line way. The proposed crack detection workflow described in Section 2.4 was applied on the set of 1596 images having cracks of different sizes and shapes. A human expert marked the right position as ground truth. They were classified as small size cracks if the widths are less than 10 pixels, middle size cracks as the range from 10 to 20 pixels and large size cracks greater than 20 pixels. The crack detection was evaluated with hit rates and coverage ratios.

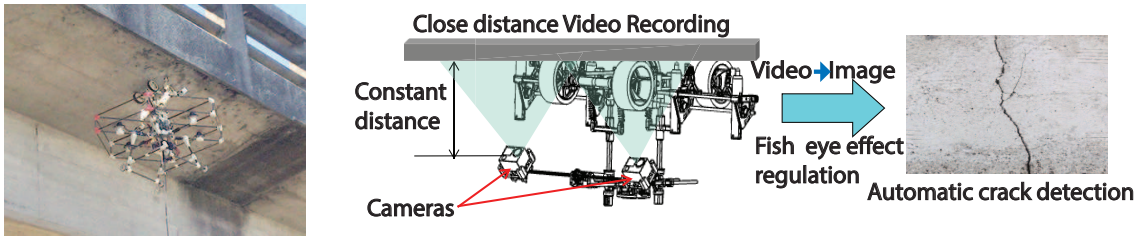

FIGURE 3. A drone based inspection system

4. **Results in Computer Experiments.** For the accuracy validation of the crack detection, the dataset of three types of images was used as explained in Section 3. As the comparative analysis, traditional methods based on the anisotropic diffusion (AD) [17], image morphology (IM) [18] and the proposed method were applied to the dataset with the ground truth, as shown in Figure 4. In the figure, results obtained by individual automatic detections and the ground truth (correct data given by the human expert) were superimposed. In the presence of chalk in the image, the anisotropic diffusion could not discriminate target cracks from chalk and other noisy data (Figure 4(a) left panel) and AD results commonly have similar tendencies to track scattered dots (Figure 4). We defined hit rates as the verification from the automatic detection to correct data (if it is unmatched, the score decreases, because the automatic detection is redundant) and coverage ratios as the verification from the correct data to automatic detection (if it is unmatched, the score decreases, because the correct date is not covered by the detection).

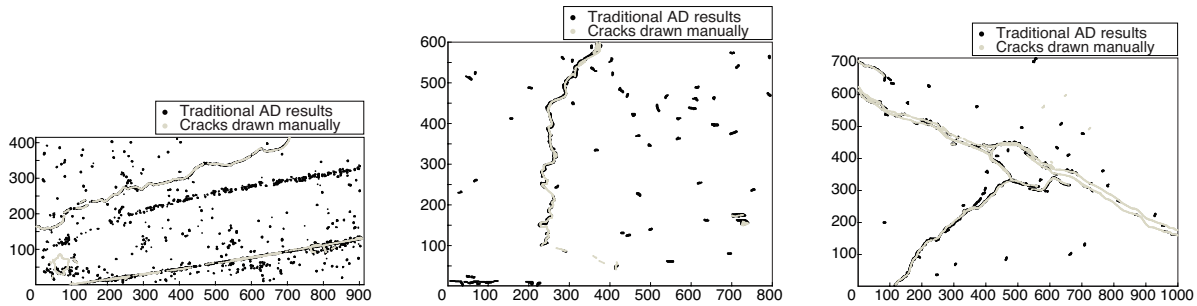

(a) Cracks detection by the anisotropic diffusion method [17] with respect to correct data

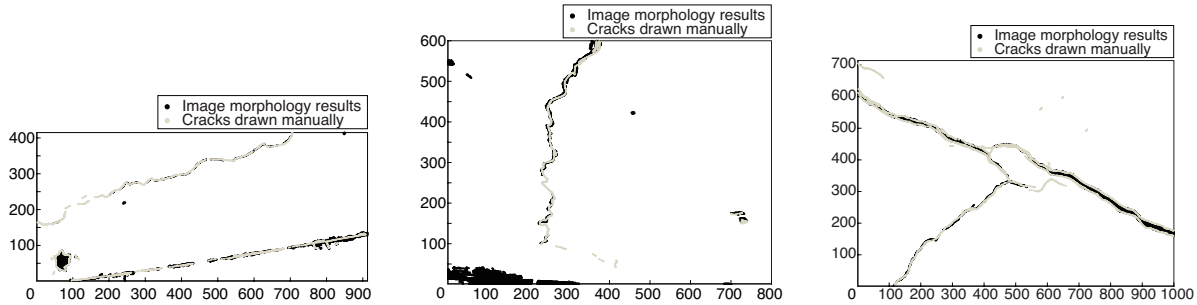

(b) Cracks detection by the image morphology method [18] with respect to correct data

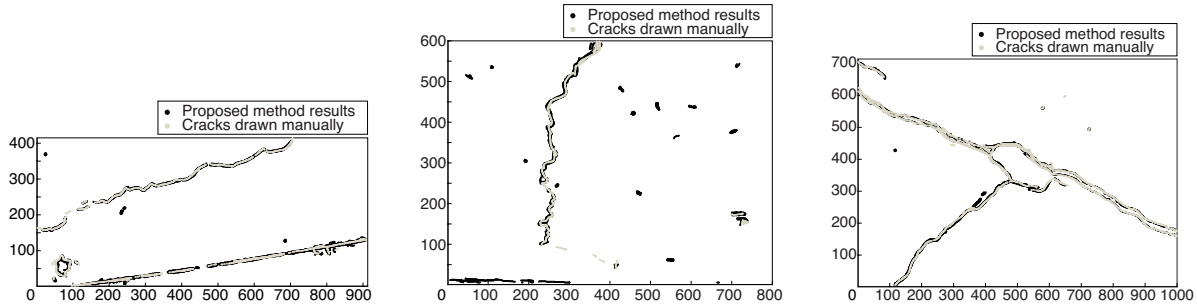

(c) Cracks detection by the proposed method with respect to correct data

FIGURE 4. Comparisons of detections of small size cracks (left), medium size cracks (center) and large size cracks (right) by different methods with respect to correct data

In this sense, AD has a high coverage ratio and a low hit rate, which means the result is redundant and unnecessary detections are happening. In the quantitative analysis with the set of 1596 images, AD, IM and the proposed method demonstrated 62.32%, 67.56% and 78.79% coverage ratios respectively for small size cracks (Figure 5(a)), 69.93%, 53.88% and 73.37% coverage ratios respectively for medium size cracks (Figure 5(b)) and 64.10%, 68.29% and 75.21% coverage ratios respectively for large size cracks (Figure 5(c)). In the quantitative analysis of hit rates, AD, IM and the proposed method demonstrated 23.61%, 29.89% and 61.58% hit rates respectively for small size cracks (Figure 5(d)), 73.42%, 44.07% and 76.63% hit rates respectively for medium size cracks (Figure 5(e)) and 54.50%, 57.86% and 62.81% hit rates respectively for large size cracks (Figure 5(f)). As a consequence of the results, the proposed method clearly demonstrated a highest accuracy in the sense of having more than 73% in coverage ratios and more than 60% hit rates in the total range of sizes. In particular, in the case of small size cracks, hit rates of other methods were less than 30%, while the proposed method exceeded the 60% hit rate, which is twice as others. Statistical tests also proved such differences of the accuracy.

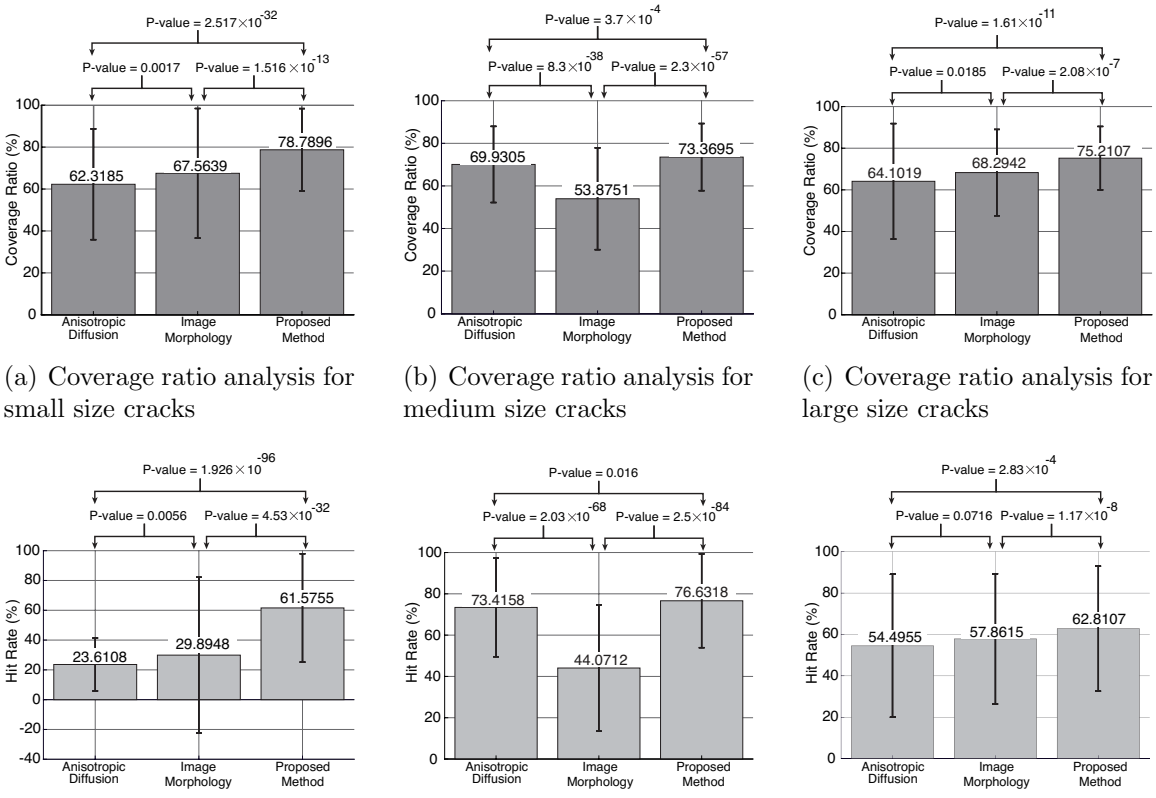

(a) Coverage ratio analysis for small size cracks

(b) Coverage ratio analysis for medium size cracks

(c) Coverage ratio analysis for large size cracks

(d) Hit rate analysis for small size cracks

(e) Hit rate analysis for medium size cracks

(f) Hit rate analysis for large size cracks

FIGURE 5. Analysis of means and standard deviations of coverage ratios and hit rates for different size cracks on different sets of images

5. **Conclusion.** Our proposed method was clearly validated whether or not it finely detects cracks on images even for less than 10 pixels in width, which normally correspond to the submillimeter range. Conventional methods and the proposed method were applied to 1596 images with cracks in different sizes. In the accuracy verification, comparisons with the ground truth demonstrated the detection efficiency of the proposed method by

showing high coverage ratios and hit rates over 60% especially in the submillimeter-width detection which were significantly different from results by conventional methods.

In recent years, due to practical research, the crack detection on the surface of concrete bridges is growing as a significant research in the field of civil infrastructure and image processing. The proposed method is applicable for finding cracks on the bridge, building and roads with potential risks and it enables to embed into not only drones but also vehicles or other mobilities for accumulating of monitoring data in a common infrastructure risk management database in the near future.

Acknowledgment. This work was supported in part by JSPS KAKENHI (16H01616, 17H06383) and the New Energy and Industrial Technology Development Organization (NEDO) and Cross-ministerial Strategic Innovation Promotion Program (SIP) "Infrastructure Maintenance, Renovation, and Management" (funding agency: NEDO).

REFERENCES

[1] M. Salman, S. Mathavan, K. Kamal and M. Rahman, Pavement crack detection using the Gabor filter, *The 16th International IEEE Conference on Intelligent Transportation Systems (ITSC2013)*, pp.2039-2044, 2013.

[2] A. Zhang, K. C. P. Wang, B. Li, E. Yang, X. Dai, Y. Peng, Y. Fei, Y. Liu, J. Q. Li and C. Chen, Automated pixel-level pavement crack detection on 3D asphalt surfaces using a deep-learning network, *Computer-Aided Civil and Infrastructure Engineering*, vol.32, no.10, pp.805-819, 2017.

[3] N. Hoang and Q. Nguyen, A novel method for asphalt pavement crack classification based on image processing and machine learning, *Engineering with Computers*, vol.35, no.2, pp.487-498, 2019.

[4] M. Islam, M. Sohaib, J. Kim and J.-M. Kim, Crack classification of a pressure vessel using feature selection and deep learning methods, *Sensors*, vol.18, no.12, DOI: 10.3390/s18124379, 2018.

[5] M. Solís, M. Algaba and P. Galvín, Continuous wavelet analysis of mode shapes differences for damage detection, *Mechanical Systems and Signal Processing*, vol.40, no.2, pp.645-666, 2013.

[6] X. Zhou, L. Xu and J. Wang, Road crack edge detection based on wavelet transform, *IOP Conference Series: Earth and Environmental Science*, vol.237, no.3, DOI: 10.1088/1755-1315/237/3/032132, 2019.

[7] Z. Zhang, O. Hamata, T. Akiduki, T. Mashimo, T. Saito and K. Hayashi, Cracks in bridge floor detected by 2-dimensional complex discrete wavelet packet transform, *International Journal of Innovative Computing, Information and Control*, vol.16, no.6, pp.2007-2019, 2020.

[8] K. C. Veluvolu, C. Ma, H. Zhang and B. K. Li, Shadow separation of pavement images based on morphological component analysis, *Journal of Control Science and Engineering*, DOI: 10.1155/2021/8828635, 2021.

[9] J.-L. Starck, Y. Moudden A, J. Bobin, M. Elad and D. L. Donoho, Morphological component analysis, *Proc. of the International Society for Optical Engineering (SPIE)*, DOI: 10.1117/12.615237, 2005.

[10] J.-L. Starck, M. Elad and D. L. Donoho, Image decomposition via the combination of sparse representations and a variational approach, *IEEE Trans. Image Processing*, vol.14, no.10, pp.1570-1582, 2005.

[11] J. Bobin, J.-L. Starck, J. M Fadili, Y. Moudden and D. L Donoho, Morphological component analysis: An adaptive thresholding strategy, *IEEE Trans. Image Processing*, vol.16, no.11, pp.2675-2681, 2007.

[12] A. Dixit and H. Wagatsuma, Investigating the effectiveness of the sobel operator in the MCA-based automatic crack detection, *2018 4th International Conference on Optimization and Applications (ICOA)*, pp.1-6, 2018.

[13] A. Dixit and H. Wagatsuma, Comparison of effectiveness of dual tree complex wavelet transform and anisotropic diffusion in MCA for concrete crack detection, *2018 IEEE International Conference on Systems, Man, and Cybernetics (SMC)*, pp.2681-2686, 2018.

[14] S. S. Chen, D. L. Donoho and M. A. Saunders, Atomic decomposition by basis pursuit, *SIAM Review*, vol.43, no.1, pp.129-159, 2001.

[15] J. J. Fuchs, More on sparse representations in arbitrary bases, *IFAC Proceedings Volumes*, vol.36, no.16, pp.1315-1320, 2003.

[16] J.-L. Starck, F. Murtagh and J. M. Fadili, *Sparse Image and Signal Processing: Wavelets, Curvelets, Morphological Diversity*, Cambridge University Press, 2010.

[17] P. Perona and J. Malik, Scale-space and edge detection using anisotropic diffusion, *IEEE Trans. Pattern Analysis and Machine Intelligence*, vol.12, no.7, pp.629-639, 1990.
[18] A. Mohan and S. Poobal, Crack detection using image processing: A critical review and analysis, *Alexandria Engineering Journal*, vol.57, no.2, pp.787-798, 2018.

Author Biography

Ankur Dixit received his Master's degree in Electronics & Communication Engineering in 2014 from National Institute of Technology (NIT), Kurukshetra, Haryana, India. He worked in the Mangalayatan University as an assistant professor in 2014-2017. He enrolled at the Ph.D. course in Kyushu Institute of Technology, Japan from 2017 and he is receiving the Ph.D. supervision.

Wataru Oshiumi is currently a fourth-grade undergraduate student in Department of Mechanical and Control Engineering, Faculty of Engineering, Kyushu Institute of Technology, Japan. He is interested in image processing systems.

Hiroaki Wagatsuma received his M.S., and Ph.D. degrees from Tokyo Denki University, Japan, in 1997 and 2005, respectively. In 2009, he joined Kyushu Institute of Technology as Associate Professor, and from December 2021 he was promoted into the Professor of Department of Human Intelligence Systems. His research interests include non-linear dynamics and robotics. He is a member of IEEE.